Amine oxidase, copper containing 3 exerts anti-mesenchymal transformation and enhances CD4+ T-cell recruitment to prolong survival in lung cancer

CHAO-YUAN CHANG[1,2], KUAN-LI WU[1,3,4], YUNG-YUN CHANG[1,3,5], PEI-HSUN TSAI[1], JEN-YU HUNG[1,3,4], WEI-AN CHANG[3,6], SHU-FANG JIAN[1], YUNG-CHI HUANG[1], INN-WEN CHONG[1,3,4], YING-MING TSAI[1,3,4,7] and YA-LING HSU[1,7]

[1]Graduate Institute of Medicine, College of Medicine, Kaohsiung Medical University; [2]Department of Anatomy, Kaohsiung Medical University; [3]Division of Pulmonary and Critical Care Medicine, Kaohsiung Medical University Hospital, Kaohsiung Medical University; [4]School of Medicine, College of Medicine, Kaohsiung Medical University; [5]Division of General Medicine, Kaohsiung Medical University Hospital, Kaohsiung Medical University; [6]Graduate Institute of Clinical Medicine, College of Medicine, Kaohsiung Medical University; [7]Drug Development and Value Creation Research Center, Kaohsiung Medical University, Kaohsiung 807, Taiwan, R.O.C.

Received November 9, 2020; Accepted June 15, 2021

DOI: 10.3892/or.2021.8154

Abstract. Lung cancer remains notorious for its poor prognosis. Despite the advent of tyrosine kinase inhibitors and immune checkpoint inhibitors, the probability of curing the disease in lung cancer patients remains low. Novel mechanisms and treatment strategies are needed to provide hope to patients. Advanced strategies of next generation sequencing (NGS) and bioinformatics were used to analyze normal and lung cancer tissues from lung cancer patients. Amine oxidases have been linked to leukocyte migration and tumorigenesis. However, the roles of amine oxidases in lung cancer are not well-understood. Our results indicated that amine oxidase, copper containing 3 (AOC3) was significantly decreased in the tumor tissue compared with the normal tissue, at both the mRNA and protein level, in the included lung cancer patients and public databases. Lower expression of AOC3 conferred a poorer survival probability across the different cohorts. Epigenetic silencing of AOC3 via miR-3691-5p caused tumor promotion and progression by increasing migration and epithelial-mesenchymal transition (EMT). Furthermore, knockdown of AOC3 caused less CD4+ T-cell attachment onto lung cancer cells and reduced transendothelial migration *in vitro*, as well as reducing CD4+ T-cell trafficking to the lung *in vivo*. In conclusion, the present study revealed that downregulation of AOC3 mediated lung cancer promotion and progression, as well as decrease of immune cell recruitment. This novel finding could expand our understanding of the dysregulation of the tumor immune microenvironment and could help to develop a novel strategy for the treatment of lung cancer.

Correspondence to: Professor Ying-Ming Tsai, Graduate Institute of Medicine, College of Medicine, Kaohsiung Medical University, 100 Shih-Chuan 1st Road, Kaohsiung 807, Taiwan, R.O.C.
E-mail: yingming@kmu.edu.tw

Abbreviations: EML4-ALK, echinoderm microtubule-associated protein-like 4-anaplastic lymphoma kinase; AOC3, amine oxidase, copper containing 3; CAO, copper-containing amine oxidase; EGFR, epithelial growth factor receptor; EMT, epithelial-mesenchymal transition; MAO, monoamine oxidase; NGS, next generation sequencings; TIME, tumor immune microenvironment; TME, tumor microenvironment

Key words: AOC3, lung cancer, EMT, microRNA-3691-5p, tumor immune microenvironment

Introduction

Lung cancer is the leading cause of cancer-related deaths worldwide with a high annual incidence and a 5-year survival rate of <20% regardless of its stage at diagnosis (1,2). However, when it metastasizes, the 5-year survival rate is less than 5% (3). Non-small cell lung cancer (NSCLC) is the most common type of lung cancer, representing ~80% of all cases (4,5). The two most prevalent NSCLC subtypes are lung adenocarcinoma (LUAD) and lung squamous cell carcinoma (LUSC), which constitute 35 and 25% of all cases, respectively (5). There have been notable advances in our understanding of lung cancer and its underlying mechanisms of action, which have been clearly elucidated and exemplified (6). There have also been marked improvements recently in the treatments available for lung cancer. The current treatment protocol consists of a platinum doublet, tyrosine kinase inhibitors for epithelial growth factor receptor (EGFR), echinoderm microtubule-associated protein-like 4-anaplastic lymphoma kinase (EML4-ALK) fusion protein and immune checkpoint inhibitors (3). However, the prognosis for lung cancer remains poor and a more detailed mechanism and treatment options are needed.

In addition to the malignant cells, the surrounding microenvironment is also critical for tumorigenesis (7,8). Amine oxidases refer to a class of enzymes that catalyze the deamination of amine groups to produce aldehydes, ammonia and hydrogen peroxide (9). There are a variety of amine oxidases consisting of four classes of monoamine oxidases (MAOs), including MAO-A and MAO-B, polyamine oxidases, lysyl oxidases, and copper-containing amine oxidases (CAOs) (10). CAOs have been revealed to participate in the regulation of a variety of pathological and physiological processes, such as cell proliferation, differentiation, glucose uptake and immune regulation (11). Changes in CAO activity are correlated with a variety of human diseases, including diabetes mellitus, Alzheimer's disease, and inflammatory disorders (12,13). The four complete genes for CAOs are amine oxidase, copper containing *(AOC)1-4*. AOC1 consists of a homodimeric glycoprotein with an apparent molecular mass of 186 kDa; it is secreted as a diamine oxidase to generate hydrogen peroxide (14,15). AOC1 is strongly expressed in the kidneys, placenta, intestine and lungs (14). Little is known about the molecular mechanisms regulating *AOC1* gene expression. The *AOC2* gene encodes retina-specific amine oxidase (16), which was originally identified in ganglion cells. Its functions remain unclear but it may play a role in hereditary retinal diseases (16). The *AOC4* gene encodes a soluble plasma amine oxidase in cows as bovine AOC4 (17) but not in humans, mice or rats. The *AOC3* gene encodes vascular adhesion protein-1, which is primarily expressed on the endothelial cell surface but also in smooth muscle cells and adipocytes (18). In addition to its amine oxidase activity, AOC3 functions as a non-classical inflammation-inducible endothelial molecule which is linked to leukocyte-subtype specific rolling under physiological shear (18). It has been revealed that the enzymatic activity of AOC3 is functionally important, and leukocyte recruitment is impaired if its activity is abolished (10).

The surrounding microenvironment of cancer contributes to its promotion and progression (19). Due to its unique tumor microenvironment (TME), cancer promotes and strengthens its own progression as a result of its interactions. The cells inside the TME include cancer-associated fibroblasts, endothelial cells and immune cells (20), which form the tumor immune microenvironment (TIME). The functions and densities of different tumor-infiltrating immune cells in the TIME are closely associated with prognosis and prediction of the treatment response (7). Therefore, there is an urgent need for improved understanding of immune dysfunction inside the TIME and the mechanisms by which the tumor modifies its environment to remove the functional immunity of the body. The present study aimed to verify the role of AOC3 in lung cancer progression and the relevant anticancer immunity.

Materials and methods

Cell lines and reagents. Murine Lewis lung carcinoma (LLC) cell line and human umbilical vein endothelial cells (HUVECs) were purchased from American Type Culture Collection (ATCC). Human lung cancer CL1-5 cells were kindly provided by Dr Pan-Chyr Yang of National Taiwan University (Taipei City, Taiwan) and were cultured in RPMI-1640 medium (Lonza Group, Ltd.) supplemented with 10% fetal bovine serum (FBS), 100 U/ml penicillin and 100 μg/ml streptomycin (Thermo Fisher Scientific, Inc.; Waltham, MA, USA) at 37˚C. Recombinant human and mouse AOC3 were obtained from R&D Systems, Inc. Knockdown of AOC3 in CL1-5 cells was performed using either pLKO_005 plasmid as a control or AOC3-shRNA plasmid (14 μg shRNA plasmid for $5x10^5$ cells in a 6-well plate) obtained from the National RNAi Core Facility (Academia Sinica, Taipei, Taiwan). The plasmid was transfected into cells using Lipofectamine 2000™ Thermo Fisher Scientific, Inc.) for 2 days, and the stable clone of AOC3-knockdown cells were established by puromycin selection (5 μg/ml). All cells were authenticated by short tandem repeat (Promega Corporation) and examined for mycoplasma contamination using a MycoAlert™ mycoplasma detection kit (Lonza Group, Ltd.) according to the manufacturer's protocol every three months.

Next generation sequencing (NGS) and bioinformatics analysis. All of the participants selected from January 2018 to December 2019, provided written informed consent prior to inclusion in the present study. The patients who agreed and received surgical intervention were enrolled in this study. The adjacent non-tumor lung and tumor tissues of ten patients (7 from LUAD and 3 from LUSC) were obtained from the Division of Thoracic Surgery and Division of Pulmonary and Critical Care Medicine, Kaohsiung Medical University Hospital (Kaohsiung, Taiwan). The protocol of the present study was reviewed and approved (approval no. KMUH-IRB-20130054 and KMUH-IRB-G(II)-20180021) by the Institutional Review Board of Kaohsiung Medical University Hospital. The deep RNA-seq was carried out at a biotechnology company (Welgene, Inc.) using the Solexa platform. RNA and small RNA library construction was carried out using a sample preparation kit (Illumina, Inc.) following the protocol of the TruSeq RNA or Small RNA Sample Preparation Guide.

The expression of AOCs in lung cancer and normal specimens (cancer vs. normal) were extracted from the Oncomine® database (http:/www.oncomine.org; Compendia Biosciences) (21) and The Cancer Genome Atlas (TCGA) cohort of UALCAN (http://ualcan.path.uab.edu/analysis.html) (22). The 16 cohorts from Oncomine® database included Su *et al* (23), Okayama *et al* (24), Landi *et al* (25), Beer *et al* (26), Stearman *et al* (27), Selamat *et al* (28), Garber *et al* (adenocarcinoma and squamous) (29), Hou *et al* (adenocarcinoma, squamous and large cell) (30), Wachi *et al* (squamous) (31), Bhattacharjee *et al* (adenocarcinoma, squamous, carcinoid and small cell) (32). Criteria in the analysis were fold change >2 and P-value $<10^{-4}$, which was calculated using the Oncomine® database through two-sided Student's t-test. The data of *AOC* mRNA, copy number and overall survival in TCGA database, and AOC protein were analyzed by UALCAN website (http://ualcan.path.uab.edu/analysis-prot.html) (22). The immunohistochemical staining for AOC3 in lung cancer and normal lung tissue samples were acquired from The Human Protein Atlas (33). The association between gene expression and clinical outcome of lung cancer patients was evaluated by publicly available data using Kaplan-Meier (K-M) plotter and log-rank testing (https://kmplot.com/analysis/) (34), UALCAN and PROGgeneV2 (35). The post-transcriptional regulation

was predicted using miRWalk (version 3.0) (36), miRanda (37) and miRDB (38) with restriction of >95% confidence.

Measurement of AOC3. All of the participants provided written informed consent prior to inclusion in the present study. The sera of 40 healthy donors and 40 lung cancer patients (healthy donors: Age range, 40-80 years old; M/F 31%/69%; lung cancer donors: Age range 30-90 years old; M/F 46/54%) were collected from the Division of Thoracic Surgery and Division of Pulmonary and Critical Care Medicine, Kaohsiung Medical University Hospital (Kaohsiung, Taiwan) from January 2018 to December 2019. The patients who agreed with written informed consent were enrolled in this study before starting definite treatment. These samples were assessed using Quantikine Human VAP-1 Immunoassay (R&D Systems, Inc.). The protocol of the present study was reviewed and approved (app roval no. KMUH-IRB-20130054) by the Institutional Review Board of Kaohsiung Medical University Hospital.

Reverse transcription-quantitative (RT-q) PCR. Total RNAs were extracted from CL 1-5 lung cancer cells with TRIzol reagent (Thermo Fisher Scientific, Inc.) and reverse transcribed into cDNA using an oligo (dT) primer and reverse transcriptase (PrimeScript RT Reagent Kit; Takara Bio, Inc.) following the manufacturer's protocols. The reaction conditions were as follows: Priming for 5 min at 25˚C, reverse transcription for 20 min at 46˚C, and final inactivation of reverse transcriptase for 1 min at 95˚C (40). The expression levels of specific genes were determined by a StepOne-Plus PCR instrument (Applied Biosystems; Thermo Fisher Scientific, Inc.), using real-time analysis with SYBR-Green (Thermo Fisher Scientific, Inc.). The following primers were used: AOC1 forward, 5'-AOC1_H_F2 GTGATGGAGGCC AAGATGCA-3' and reverse, 5'-AOC1_H_R2 TCTGCAGTG TCTGGAAGCTG-3'; AOC2 forward, 5'-AOC2_H_F2 GCC TTCCACTTCAAGCTGGA-3' and reverse, 5'-AOC2_H_R2 GCTCTCAGGTCCTCCTTTCC-3'; AOC3 forward, 5'-AOC3_H_F2 GTGGGGCCATAGAAATACGA-3' and reverse, 5'-AOC3_H_R2 CAGACCCAGTTCTCCAGTCC-3'; and glyceraldehyde-3-phosphate dehydrogenase (GAPDH) forward, 5'-TTCACCACCATGGAGAAGGC-3' and reverse, 5'-GGCATGGACTGTGGTCATGA-3'. The RT-qPCR was performed at 95˚C for 20 sec, followed by 40 cycles at 95˚C for 5 sec and 60˚C for 35 sec (39). Relative expression levels of the cellular mRNA were normalized to GAPDH. The relative standard method ($2^{-\Delta\Delta Cq}$) was used to calculate relative RNA expression (40).

Cell proliferation and 5-bromo-2-deoxyuridine (BrdU) incorporation. Cells ($3x10^3$ cells/well) were seeded in a 96 well plate, and then cultured for 48 or 72 h. Cell proliferation was determined by cell proliferation reagent WST-1 proliferation assay kit (Takara Bio, Inc.) after 2-h incubation and measured at a 450-nm wavelength according to the manufacturer's instructions. Cells were labelled with BrdU (10 μM) at day 2 after seeding followed by fixation. In the BrdU incorporation assay, cells were fixed at room temperature for 30 min with 200 μl/well of the Fixing Solution (included in the kit undermentioned) and incubated at room temperature for 30 min. Integrated BrdU was assessed by ELISA-based method according to the manufacturer's protocol (BrdU Cell Proliferation Assay Kit; cat. no. 2750; EMD Millipore).

Wound healing analysis. CL 1-5 cells were seeded into a 12 well-pate at 90% confluence and cultured in 1% of FBS-containing medium for exogenous AOC3 (control, 10, 20 and 50 ng/ml) and 10% of FBS-containing medium (since cell proliferation was not affected by AOC3 knockdown, in order to mimic the physiologic conditions, 10% of FBS-containing medium was used and cells were not serum starved) for AOC3-shRNA knockdown at 37˚C as previously described by Shao *et al* (41), and the cell migration was evaluated by measuring the migration of cells into the acellular region formed by a sterile yellow tip. The wound closure was observed after 8 h. The wound healing assay was closely observed via a Nikon inverted microscope (Nikon Corporation).

$CD4^+$ T-cell isolation. Peripheral blood mononuclear cells (PBMCs) of healthy donors (eight healthy donors: Age range, 35-45 years old; male only) were obtained from the Division of Pulmonary and Critical Care Medicine, Kaohsiung Medical University Hospital (Kaohsiung, Taiwan) from January 2020 to December 2020. The protocol of the present study was reviewed and approved (approval no. KMUH-IRB-20130054) by the Institutional Review Board of Kaohsiung Medical University Hospital and the donors provided written informed consent. PBMCs were isolated using 7.5 ml Ficoll-Hypaque gradient reagent (EMD Millipore) in 1 ml blood mixing with 5 ml PBS, and human $CD4^+$ T cells were isolated form PBMC using $CD4^+$ T-cell Isolation Kit (MACS MicroBeads; Miltenyi Biotec GmbH) according to the manufacturer's instructions.

Cell adhesion and transendothelial migration. For transendothelial migration, HUVECs ($5x10^4$) were seeded onto inserts with polyester membranes of 3-μm pore size (EMD Millipore) and cultured at 37˚C for 48 h to form a 100% confluent monolayer. CL1-5 ($1x10^5$) or AOC3-knockdown CL1-5 ($1x10^5$) cells were seeded in the bottom of a 24-well plate containing RPMI-1640 culture medium. PKH26-labeled (EMD Millipore) $CD4^+$ T-cells were seeded onto HUVEC-coated inserts, which were placed in the wells of the 24-well plate and then incubated for 24 h at 37˚C. The migratory cells were visualized in four randomly selected fields using a Nikon fluorescence microscope (Nikon Corporation).

Western blot analysis. Total proteins from primary tissues and cell lines were extracted using RIPA lysis buffer (Thermo Fisher Scientific, Inc.). An equal amount of total protein (2 μg) was quantitated by bicinchoninic acid (BCA) analysis and separated by SDS-PAGE (6-8%). After transferring, the PVDF membranes containing bound proteins were blocked at room temperature for 2 h using 5% milk containing TBST buffer (0.02% Tween-20) and then incubated overnight at 4˚C with primary antibodies against a specific target protein. After incubation with HRP-coupled secondary antibodies (1:5,000; anti-mouse, 7076; anti-rabbit, 7074; Cell Signaling Technology) at room temperature for 1 h, the protein bands were visualized using ECL (EMD Millipore) and detected using a FluorChem HD2 System (ProteinSimple). The following primary

antibodies were used: E-cadherin (1:500; cat. no. 610182) N-cadherin (1:500; cat. no. 610921) and vimentin (1:500; cat. no. 550513; all from BD Biosciences), Slug (1:500; product no. 9585S; Cell Signaling Technology, Inc.), and GAPDH (1:5,000; cat. no. MAB374; EMD Millipore). The quantitation of the results of the western blotting was performed using AlphaImager software (Version 6.0.0; ProteinSimple).

miRNA mimics transfection. CL1-5 cells were transfected with microRNA (miR)-3691-5p (AGUGGAUGAUGGAGA CUCGGUAC; at a concentration of 100 nM; GE Healthcare Dharmacon, Inc.) or scrambled control (negative control 1; UCACAACCUCCUAGAAAGAGUAGA; at a concentration of 100 nM; GE Healthcare Dharmacon, Inc.) by using Dharmafect reagent 4 (GE Healthcare Dharmacon, Inc.) according to the manufacturer's instructions. The transfection efficacy was monitored by transfecting siGLO fluorescent oligonucleotides (catalog ID: D-001630-02-05; GE Healthcare Dharmacon, Inc.) concurrently after 24 h of transfection at 37˚C according to the manufacturer's protocol. The expression of AOC1-3, cell migration and $CD4^+$ T-cell migration as well as adhesion were assayed after a 48-h transfection.

Mouse studies. All mice procedures were approved by and conducted in accordance with the Institutional Animal Care and Use Committee at Kaohsiung Medical University (IACUC Approval No. 107104; Kaohsiung, Taiwan). C57BL/6 mice (12 males in total; weight, 18±2 g; 5 weeks old) were obtained from the Taiwan National Laboratory Animal Center (Taipei City, Taiwan). The mice were housed in a specific pathogen-free environment with the room temperature being maintained at ~20˚C, the humidity at ~45% and a 12-h light/dark cycle. Each mouse had free access to food and water. The mice were subjected to implantation of LLC cells ($1x10^6$ cells) via tail vein and tumor growth in the lungs was allowed for 7 days. Mice were treated with PBS or recombinant mouse (rm) AOC3 twice (10 μg/mouse; on days 7 and 14) by intra-tracheal route. At the end of the experiment, the mice were euthanized by CO_2 asphyxiation during which the CO_2 gas flow rate displaced 10 to 30% of the cage volume per minute. $CD4^+$ T cells of the lungs of mice were isolated by mouse $CD4^+$ T cell isolation kit (MACS MicroBeads; Miltenyi Biotec GmbH) according to the manufacturer's instructions and counted after 21 days of LLC implantation. Lung tissue was collected and minced and incubated in RPMI-1640 medium with collagenase type 1 (400 U/ml; Worthington Biochemical Corporation) at 37˚C for 1 h. The digested tissues were filtered through a 70-μm cell strainer and washed with RPMI-1640 medium. $CD4^+$ T cells of the lung filtered solution were isolated by mouse CD4 isolation kit and counted after 21 days of LLC implantation.

Statistical analyses. Each experiment was repeated at least three times. Data are expressed as the mean ± standard deviation (SD) using GraphPad Prism version 7.04 (GraphPad Software, Inc.). Two treatment groups were compared by unpaired Student's t-test. Multiple group comparisons were performed by two-way analysis of variance with Tukey's post hoc test. $P<0.05$ was considered to indicate a statistically significant difference.

Results

AOC3 mRNA expression is reduced in lung cancer. The controversial roles of AOCs have been reported in various cancer types (41-44), therefore their effect in lung cancer was investigated. Tumor tissue and adjacent normal tissue specimens from 10 lung cancer patients (7 LUAD and 3 LUSC) were analyzed via NGS (Table I). The expression of *AOC2* (7 out of 10) and *AOC3* (8 out of 10) was lower in most of the tumor tissue of patients compared with their normal tissue, however lower *AOC1* in tumor tissue was observed in only 2 out of 10 patients with lung cancer (Fig. 1A-C). Using Oncomine® datasets, it revealed that *AOC3,* but not *AOC1* or *AOC2*, was expressed at lower levels in tumor tissue compared with normal tissue in 16 lung cancer cohorts (Fig. 1D). Further analysis of these 16 cohorts revealed that the expression of *AOC3* mRNA was lower in the tumor tissue for both the LUAD and non-adenocarcinoma patients (Fig. 1E). The expression of *AOC2* and *AOC3* in LUAD and LUSC was also retrieved from TCGA cohorts. Overall *AOC2* (Fig. 1F) and *AOC3* (Fig. 1G) expression was significantly lower in the tumor tissue compared with the adjacent normal tissue, even though this trend was not observed for all stages. Moreover, the expression of *AOC3* was significantly lower in the N1 group (with lymph node metastasis) compared with the N0 group (without lymph node metastasis), implying that AOC3 may contribute to cancer metastasis (Fig. 1F and G).

AOC3 protein expression is inversely associated with lung cancer grade. AOC protein expression was extracted from the National Cancer Institute Clinical Proteomic Tumor Analysis Consortium (CPTAC). AOC1 protein expression did not vary between the tumor and normal tissue for the different types of LUAD, grades or stages (Fig. 2A-D). However, AOC3 protein expression was lower in the tumor tissue compared with the normal tissue in every cell type (Fig. 2E and F). Moreover, AOC3 expression was negatively associated with the grades and stages (early and late) of LUAD (Fig. 2G and H). The soluble form of AOC3 has been detected in other cancer types such as colorectal cancer (41). To evaluate the role of soluble AOC3 in lung cancer, serum from lung cancer patients was collected. Soluble AOC3 in the sera from lung cancer patients was lower than in healthy donors (Fig. 2I). In addition, the public datasets for the expression of AOC3 in lung cancer were utilized. Compared with normal tissue, both LUAD and LUSC expressed lower levels of AOC3 from The Human Protein Atlas (Fig. 2J). The combination of these results and the mRNA expression results indicated that AOC3 could be a promising tumor suppressor in lung cancer.

Lower expression of AOC3 confers a poorer survival time. Since the tumor tissue of lung cancers expressed lower levels of *AOC3*, its prognostic vaule in patients was evaluated by survival analysis. There are several public websites that evaluate survival analysis, including the K-M plotter, UALCAN and PROGgeneV2. According to the K-M plotter, low *AOC1* expression did not confer a poorer survival time, and it actually conferred a longer survival time in LUAD but not in LUSC patients (Fig. 3A; upper panel). *AOC2* revealed the same pattern in both types of lung cancer (Fig. 3A; middle

Table I. Characteristics of patients.

Group	Number	Sex	Age	Pathological diagnosis	Stage	T	N	M
I	01	M	70	Adenocarcinoma grade 3	2B	3	0	0
	02	M	66	Adenocarcinoma grade 3	4B	2a	0	1c
	03	F	51	Adenocarcinoma grade 3	1B	2a	0	0
	04	M	53	Adenocarcinoma grade 3	3A	3	2	0
	05	F	60	Adenocarcinoma grade 2	1A	1b	0	0
	06	M	67	Adenocarcinoma grade 1	1A	1a	0	0
	07	M	60	Adenocarcinoma grade 3	4A	4	1	1a
II	08	M	84	Squamous cell carcinoma grade 2	2B	3	0	0
	09	F	65	Squamous cell carcinoma grade 2	3A	4	0	b
	10	M	69	Squamous cell carcinoma grade 2	2B	2b	1	0

panel). However, analysis of *AOC3* expression revealed that the lower the *AOC3* expression was, the shorter the survival time was in LUAD patients but not in LUSC patients (Fig. 3A, lower panel). Moreover, the clinical implication of *AOC3* expression as detemined by survival rates was validated by cohorts extracted from the UALCAN and PROGgeneV2 websites; low expression of *AOC3* conferred a shorter surivival time but this was not observed for *AOC1* (*ABP1*) or *AOC2* (Fig. 3B and C). These results confirmed that AOC3 was strongly associated with clinical outcomes in lung cancer patients (Fig. 3A and B, lower panel; Fig. 3C).

Mechanism regulating the expression of AOC3. Since AOC3 was revealed to be critical in the prognosis of lung cancer patients, the dysregulation of AOC3 required investigation. Genetic modifications, as DNA copy number variation, DNA methylation, and post-transcriptional regulation by miRNAs were utilized. As determined by the TCGA cohort, variation in the DNA copy number of AOC3 was not correlated with the expression of *AOC3* mRNA (R=-0.121; Fig. 4A). In addition, DNA methylation of AOC3 was not significantly associated with the expression of *AOC3* mRNA (R=-0.034; Fig. 4B). Concerning post-transcriptional regulation, the miRNAs that epigenetically regulate *AOC3* mRNA were predicted using miRWalk version 3.0 with miRanda and miRDB restrictions of >95% confidence. There was a total of 27 miRNAs listed as potential regulators of the *AOC3* (Fig. 4C). This list of miRNAs was validated using the TCGA cohort and the ones with the highest probability were miR-3190 and miR-3691 since both of them had significantly increased expression in the tumor tissue compared with the normal tissue (Fig. 4D and E). Both of the predicted and highly probable miRNAs were verified in 10 lung cancer patients. The most likely miRNA to contribute to the regulation of *AOC3* mRNA was miR-3691-5p because there was an undetectable read number in most specimens for miR-3190 in our samples (Fig. 4F and G).

Low AOC3 expression mediates epithelial-mesenchymal transition (EMT) in lung cancer. Low levels of AOC3 expression conferred poor clinical outcomes in lung cancer patients. Therefore, the present study set out to verify the mechanisms by which AOC3 mediated lung cancer progression. AOC3 expression was knocked down in the LUAD cell line (CL1-5) via the shRNA method with >50% efficiency (Fig. 5A). The cells were then studied to evaluate the effect of AOC3 knockdown on proliferation. Neither the WST-1 nor the BrdU assay indicated that AOC3 affected cell proliferation in lung cancer (Fig. 5B and C, respectively). Cell migration as evaluated via wound healing analysis, revealed enhanced healing (increased migration ability) after AOC3 knockdown (Fig. 5D). In addition, AOC3 knockdown enhanced the mesenchymal characteristics as N-cadherin, vimentin and Slug were increased (Fig. 5E). The rmAOC3 protein (rhAOC3) was added to confirm the observed changes in proliferation and migration. The proliferation did not change even at a high dose (50 ng/ml) of rhAOC3 as evaluated by either WST-1 or BrdU assays (Fig. 5F and G, respectively). Cell migration was reduced after the addition of rhAOC3 in a dose-dependent manner as revealed in the wound-healing assay (Fig. 5H). The mesenchymal characteristics transitioned to epithelial features as E-cadherin was increased and N-cadherin, vimentin and Slug were decreased in a dose-dependent manner (Fig. 5I). The aforementioned results indicated that reduced AOC3 expression played a role in lung cancer progression by increasing cell migration and EMT but not proliferation.

Lung cancers with low levels of AOC3 fail to recruit CD4$^+$ T cells to the tumor in vitro and in vivo. CD4$^+$ T-cell infiltration is a critical factor for determining the TIME against cancer (26). The role of AOC3 in the recruitment of CD4$^+$ T cells remains unclear in lung cancer. To validate the role of AOC3 in mediating the TIME in lung cancer, *in vitro* and *in vivo* studies were performed. CD4$^+$ T-cell migration and attachment to lung cancer cells were evaluated. As determined by a cell adhesion assay, CD4$^+$ T-cell attachment to lung cancer cells (CL1-5) was decreased after AOC3 knockdown (Fig. 6A). Before CD4$^+$ T cells arrive at tumor sites, they must traverse the endothelia. A transendothelial migration assay was utilized to reveal the transit of CD4$^+$ T cells through the vascular endothelia. When AOC3 was silenced in cancer cells, CD4$^+$ T-cell migration was reduced, (Fig. 6B) indicating that the lower the AOC3 expression, the fewer CD4$^+$ T cells were recruited. Conversely, when rhAOC3 was added, more CD4$^+$ T cells attached to the

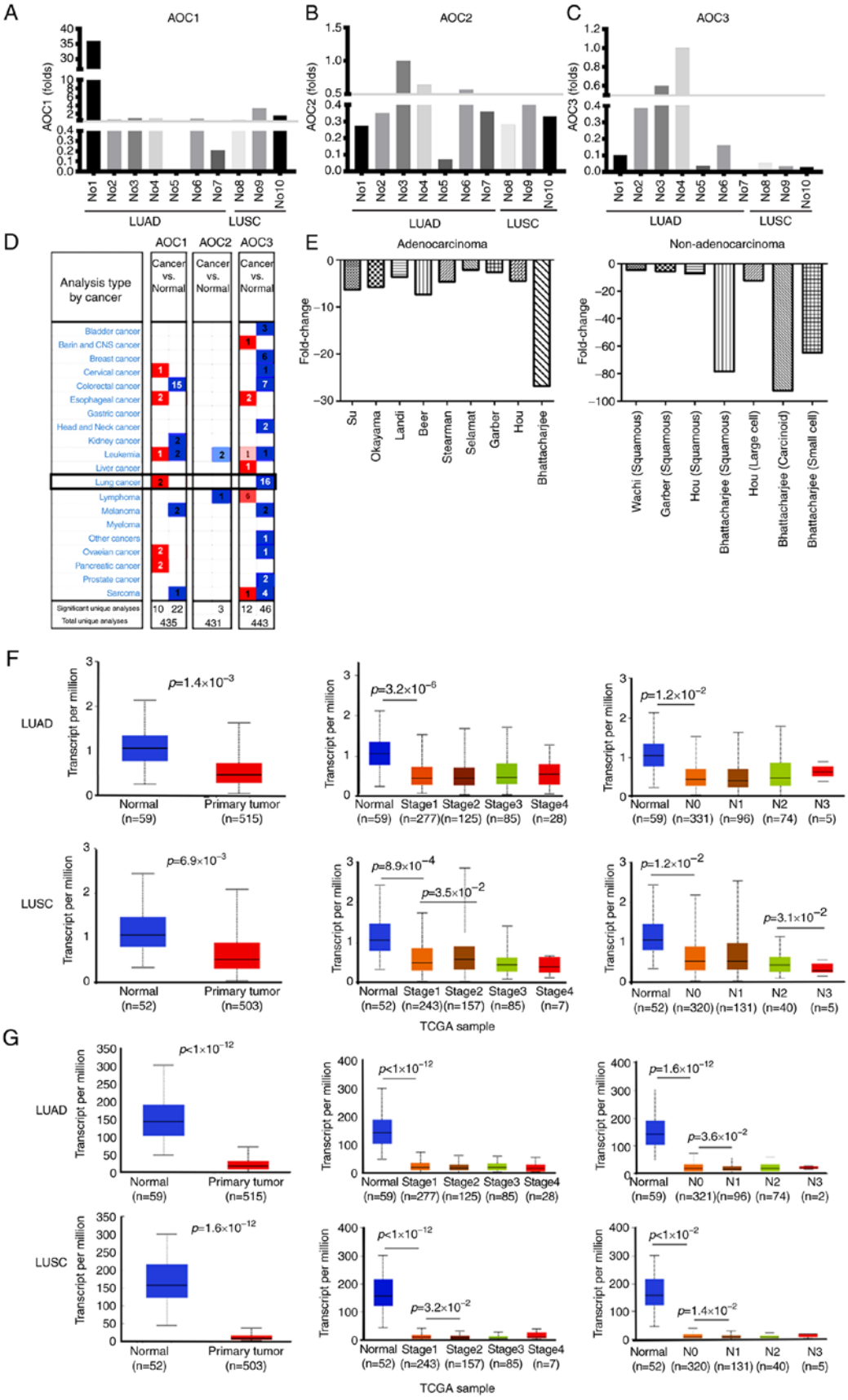

Figure 1. *AOC* mRNA expression in lung cancer. The expression of *AOCs* in the normal and tumor tissue was obtained from 10 lung cancer patients (7 LUAD and 3 LUSC). The expression of (A) *AOC1*, (B) *AOC2* and (C) *AOC3* between the tumor and normal tissue in lung cancer patients. (D) Based on the Oncomine® datasets, there was lower expression of *AOC3* in the tumor tissue compared with the normal tissue in 16 cohorts. (E) *AOC3* expression was lower in the tumor tissue compared with the normal tissue in the adenocarcinoma and non-adenocarcinoma cohorts. Furthermore, data from The Cancer Genome Atlas cohort revealed that there was lower (F) *AOC2* and (G) *AOC3* expression in the tumor tissue compared with the normal tissue in both LUAD and LUSC cohorts. Furthermore, there was lower expression of *AOC3* in the N1 group compared with the N0 group but not in all stages of lung cancer. AOC, amine oxidase, copper containing 3; LUAD, lung adenocarcinoma; LUSC, lung squamous cell carcinoma.

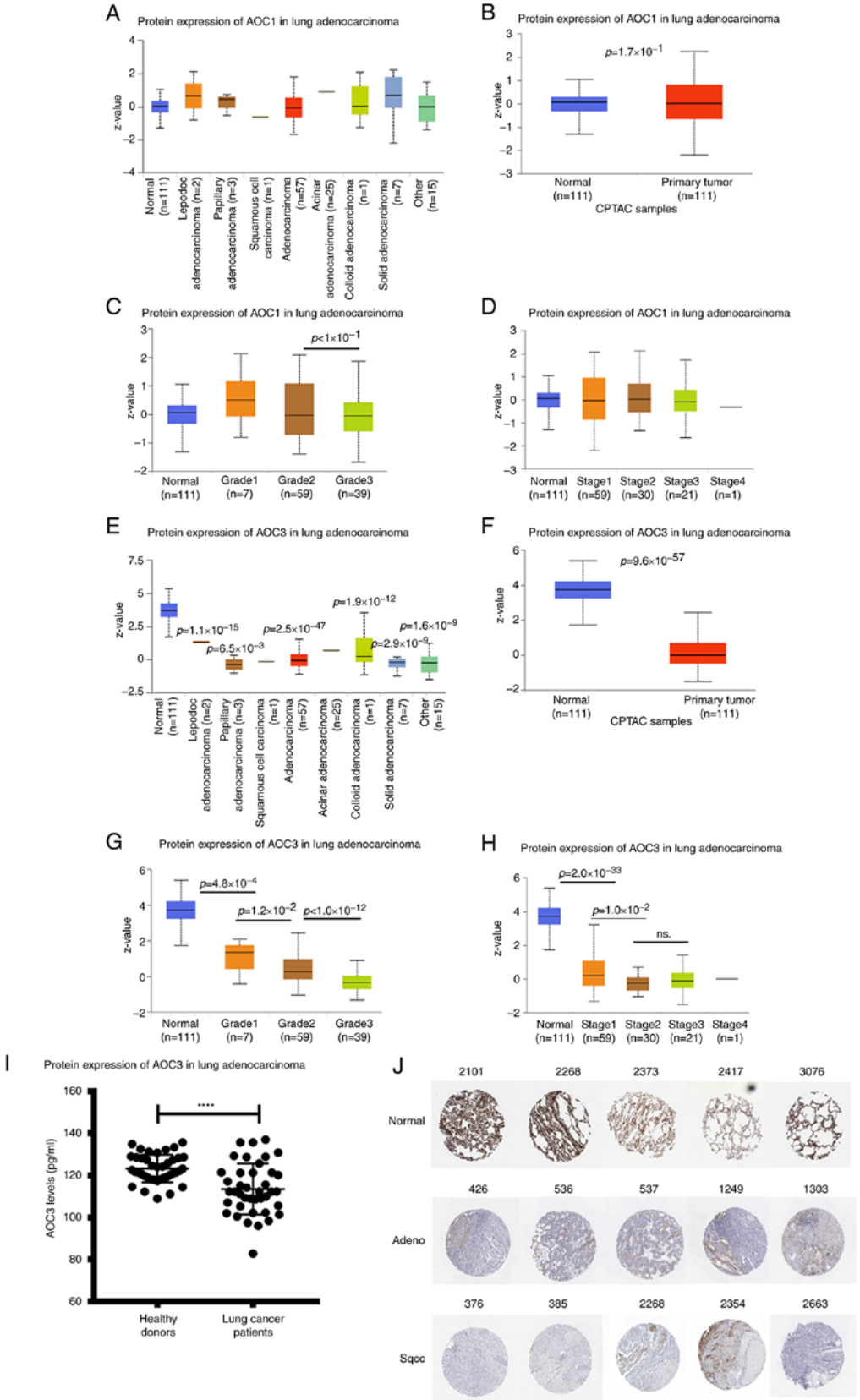

Figure 2. AOC protein expression in lung cancer. The protein expression of the AOCs was extracted from the National Cancer Institute Clinical Proteomic Tumor Analysis Consortium. Only AOC1 and AOC3 were available in this dataset. (A) The protein expression of AOC1 in lung cancer tissue vs. normal tissue was not different in lung cancer (regardless of lung cancer type), (B) lung adenocarcinoma only, (C) different grades of lung adenocarcinoma, or (D) different stages of lung cancer. (E) Conversely, the expression of AOC3 was lower in tumor tissue compared with the normal tissue in lung cancer (regardless of lung cancer type), (F) in different types of adenocarcinoma cohorts, (G) different grades of lung adenocarcinoma and (H) different stages of lung cancer. To further validate the soluble form of AOC3 in lung cancer, the sera from 40 lung cancer patients and 40 normal controls were analyzed. (I) Soluble AOC3 expression was lower in the lung cancer patients compared with the normal controls. (I) The AOC3 protein expression was also retrieved from the Human Protein Atlas. (J) The protein expression of AOC3 was attenuated in both adenocarcinoma and squamous cell carcinoma compared with normal lung tissue. ****P<0.0001. AOC, amine oxidase, copper containing 3.

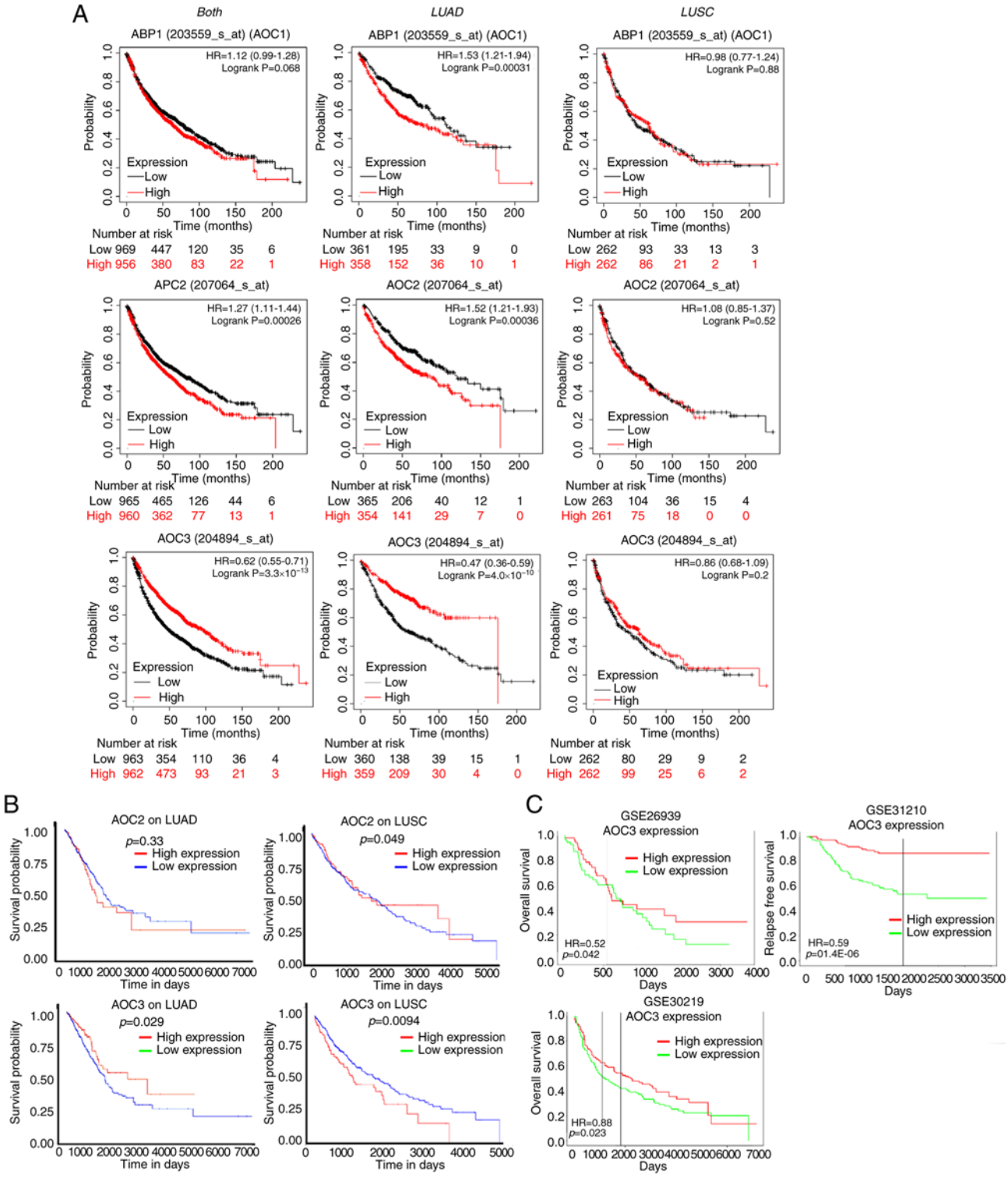

Figure 3. Survival analysis of AOCs in lung cancer. The survival time for lung cancer patients from cohorts with different levels of *AOC1*, *2* and *3* expression were further analyzed. In the Kaplan-Meier plotter, survival time was analyzed for 'both, LUAD and LUSC', 'LUAD' and 'LUSC' (from left to right). (A; upper panel) For *AOC1*, the high-expression group was associated with a shorter survival time compared with the low-expression group. (A; middle panel) For *AOC2*, the high-expression group was not associated with a longer survival time compared with the low-expression group. (A; lower panel) However, for *AOC3*, the low-expression group was associated with a shorter survival time in lung adenocarcinoma. (B) In addition, UALCAN cohorts also indicated that low expression of *AOC3* but not *AOC2* was associated with a shorter survival time compared with high expression. (C) The low expression of *AOC3* also conferred shorter survival time in different lung adenocarcinoma (GSE26919 and GSE31210) and lung cancer (GSE30219) cohorts in the PROGgeneV2. AOC, amine oxidase, copper containing 3; LUAD, lung adenocarcinoma; LUSC, lung squamous cell carcinoma.

lung cancer cells (Fig. 6C). The addition of rhAOC3 increased $CD4^+$ T-cell migration through the vascular endothelial cells (Fig. 6D). These results indicated that AOC3 increased the recruitment of $CD4^+$ T cells to lung cancer sites. AOC3 facilitation of $CD4^+$ T-cell recruitment was validated using an animal model. The *in vivo* study investigated the number of

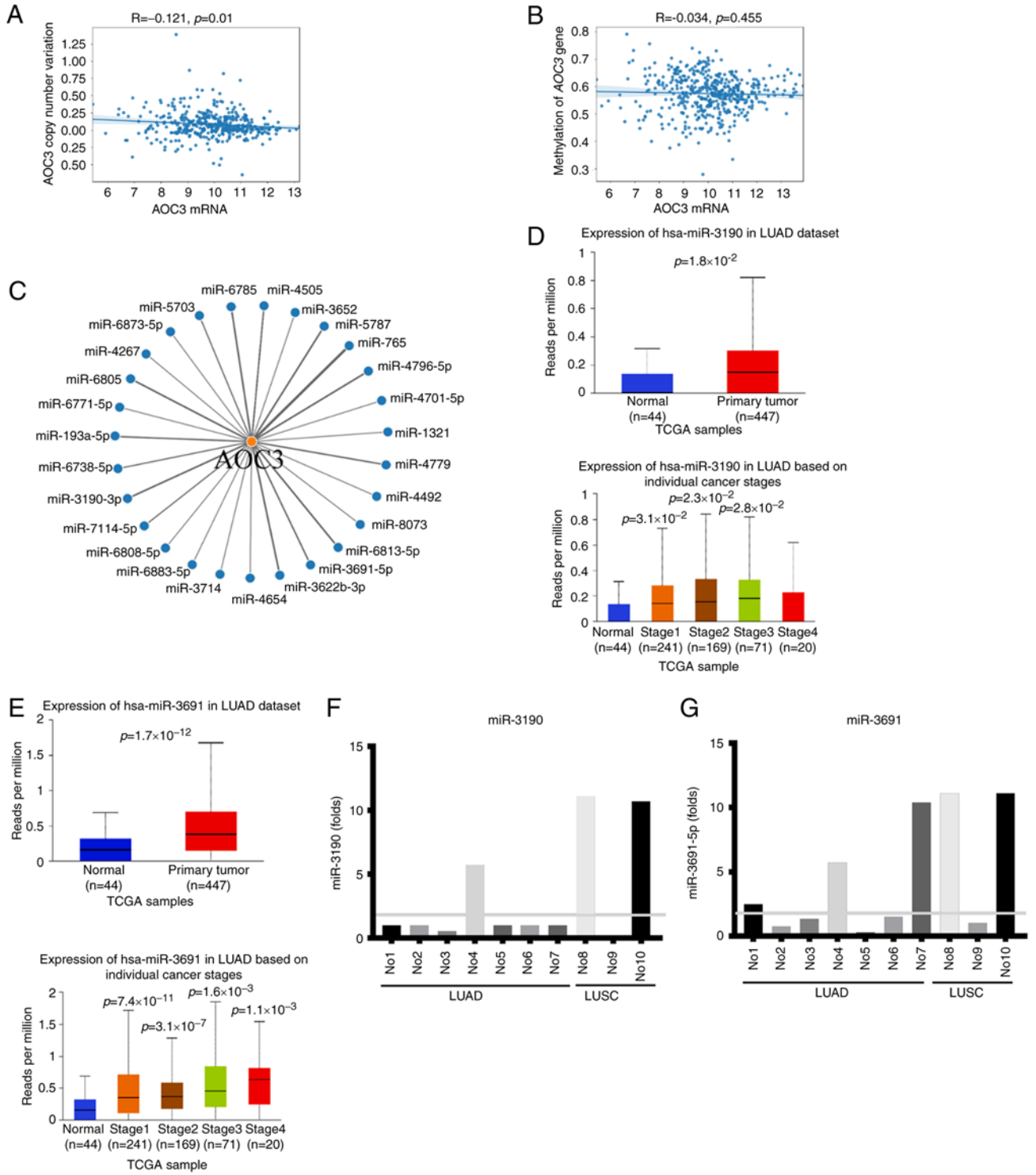

Figure 4. Regulation of *AOC3* mRNA expression. The expression of *AOC3* mRNA was regulated by genetic modifications. The TCGA cohort was used to investigate these modifications. (A) The DNA copy number of *AOC3* was not correlated with *AOC3* mRNA expression. (B) Moreover, epigenetic regulation, such as *AOC3* DNA methylation was not associated to *AOC3* mRNA expression. (C) MiRNA regulation of *AOC3* mRNA was predicted using miRWalk 3.0, and the 27 possible candidate miRNAs are listed. The present study validated the possibility of each miRNA using the TCGA cohort. The most likely candidate miRNAs included (D) miR-3190 and (E) miR-3691. Furthermore, the expression levels of indicated miRs were associated with the stages respectively. (F and G) These 2 miRNAs were further verified by data from 10 patients (including 7 lung adenocarcinoma and 3 lung squamous cell carcinoma). AOC, amine oxidase, copper containing 3; TCGA, The Cancer Genome Atlas; miR, microRNA; LUAD, lung adenocarcinoma; LUSC, lung squamous cell carcinoma.

$CD4^+$ T cells in the lungs of mice with tumors and revealed that the number of $CD4^+$ T cells was increased after rmAOC3 was instilled two times (10 μg/mouse) (Fig. 6E). These results indicated that AOC3 promoted $CD4^+$ T-cell recruitment into the TIME.

miR-3691-5 regulates EMT and cancer migration via epigenetic downregulation of AOC3. To further verify the possible regulatory role of miR-3691-5p in *AOC3* expression, miR-3691 mimics were transfected to CL1-5 cells and then their biological functions were assessed. The transfection efficacy of miRNA

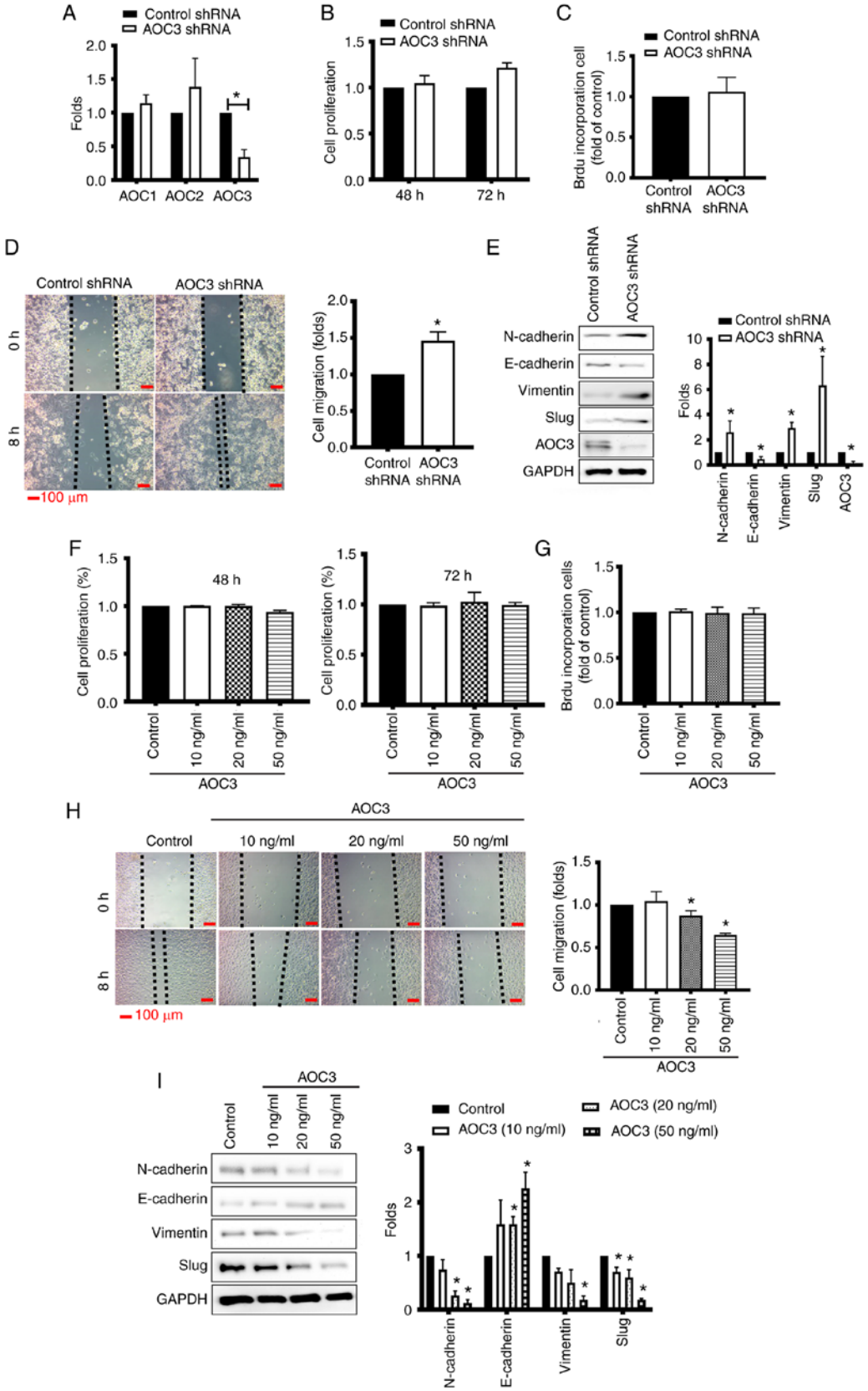

Figure 5. AOC3 mediates EMT in lung cancer. The present study investigated the mechanisms by which low AOC3 expression conferred a poor lung cancer prognosis. (A) AOC3 shRNA was used to knockdown AOC3 expression in CL1-5 cells. The knockdown efficiency was >50%. Cell proliferation was not altered as determined by (B) WST-1 and (C) BrdU incorporation assays. (D) Migration potential as determined via a wound-healing assay was enhanced after AOC3 knockdown. (E) The EMT phenomenon shifted towards the mesenchymal characteristics as indicated by increased N-cadherin, vimentin and Slug and decreased epithelial characteristics as indicated by E-cadherin. Conversely, using rhAOC3, the present study confirmed that AOC3 did not reduce cellular proliferation as revealed by (F) WST-1 and (G) BrdU incorporation assays. (H) The wound healing assay also revealed a reduction in migration potential in a dose-dependent manner after the addition of rhAOC3. (I) Concurrently, the EMT characteristics were reversed to epithelial characteristics as E-cadherin was increased and N-cadherin, vimentin and Slug were decreased. All experiments were performed independently at least three times. *P<0.05. AOC, amine oxidase, copper containing 3; EMT, epithelial-mesenchymal transition; sh-, short hairpin; BrdU, 5-Bromo-2-deoxyuridine; rh-, recombinant human.

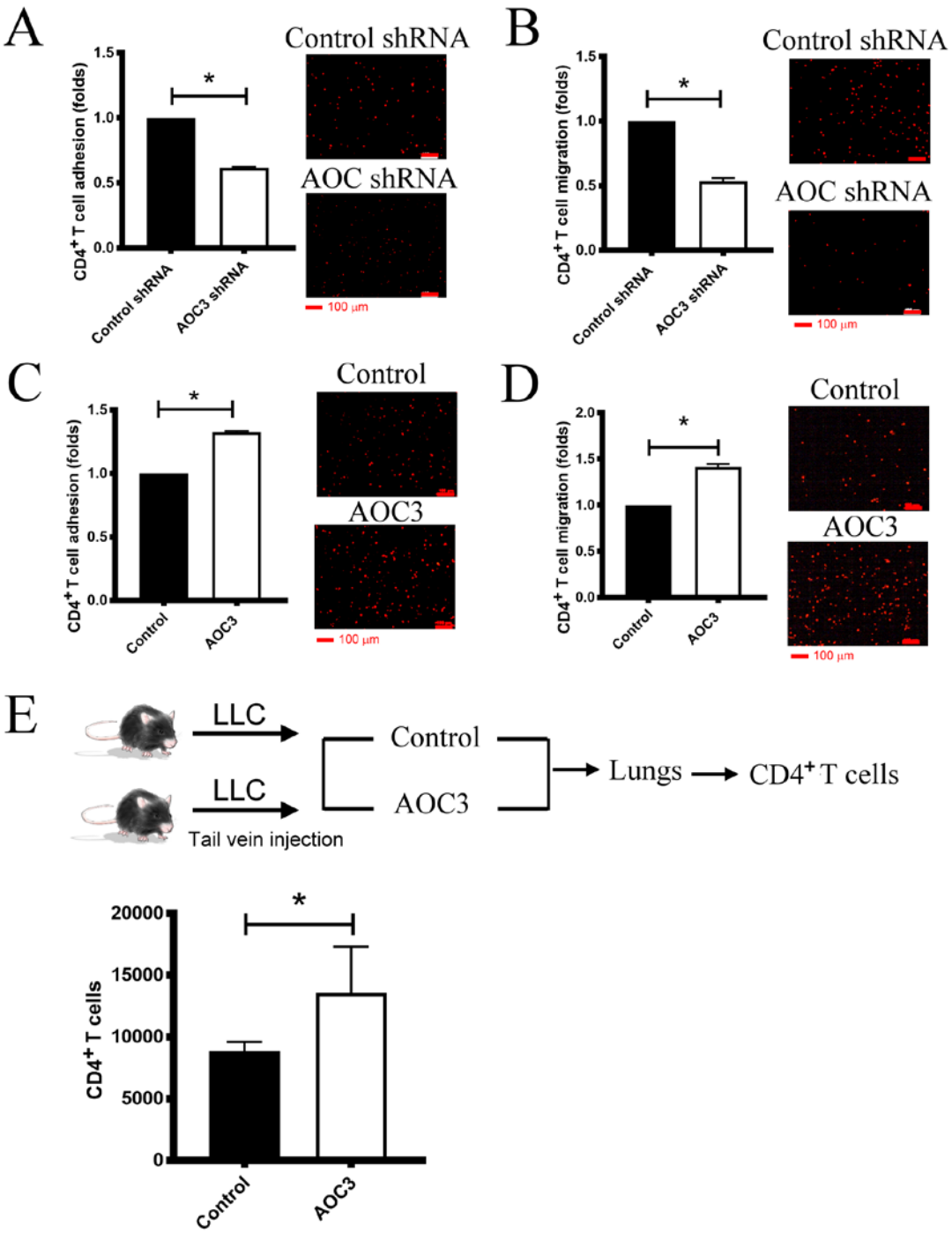

Figure 6. AOC3 attracts CD4+ T cells to lung cancer sites. The present study attempted to clarify the role of AOC3 in the recruitment of CD4+ T cells in lung tumors. The *in vitro* study used 'cell adhesion' of CD4+ T cells on lung cancer cells. After AOC3 knockdown, PKH26-stained CD4+ T cells were added to the fully-recovered lung cancer cells (CL1-5). (A) When compared with the control, the AOC3-knockdown lung cancer cells were less likely to be attached to by CD4+ T cells. (B) Moreover, the transendothelial migration assay revealed that less CD4+ T cells were attracted to AOC3-knockdown lung cancer cells compared with the control group. However, rhAOC3 increased CD4+ T-cell (C) attachment and (D) migration. Furthermore, the *in vivo* study utilized a mouse model to verify the *in vitro* findings. Lewis lung carcinoma cells were injected into mice via their tail vein. Concurrently, rmAOC3 (10 μg/mouse) was instilled into the trachea of mice twice, 7 days apart (on day 7 and day 14) (intratracheal instillation). After 14 days (day 21), the mice were sacrificed and the lungs were minced. The CD4+ T cells were then isolated. (E) The CD4+ T cells in the mice instilled with rmAOC3 were increased compared with the controls. All experiments were performed independently at least three times. *P<0.05. AOC, amine oxidase, copper containing 3; rm, recombinant mouse; LLC, Lewis lung carcinoma.

mimics was monitored by Dharmacon™ siGLO™ transfection indicators and the results revealed that >90% efficacy was achieved (Fig. 7A). miR-3691-5p downregulated expression of *AOC3* but not of *AOC1* and *AOC2* (Fig. 7B). The transfected lung cancer cells were then adopted for wound healing analysis and revealed enhanced healing process in a dose-dependent manner (increased migration ability) (Fig. 7C). Moreover, with miR-3691-5p transfection, AOC3 protein expression was decreased whereas the expression of the mesenchymal markers N-cadherin, vimentin and Slug were increased (Fig. 7D). These results indicated that miR-3691-5p affected cell migration and EMT through *AOC3*. Furthermore, to

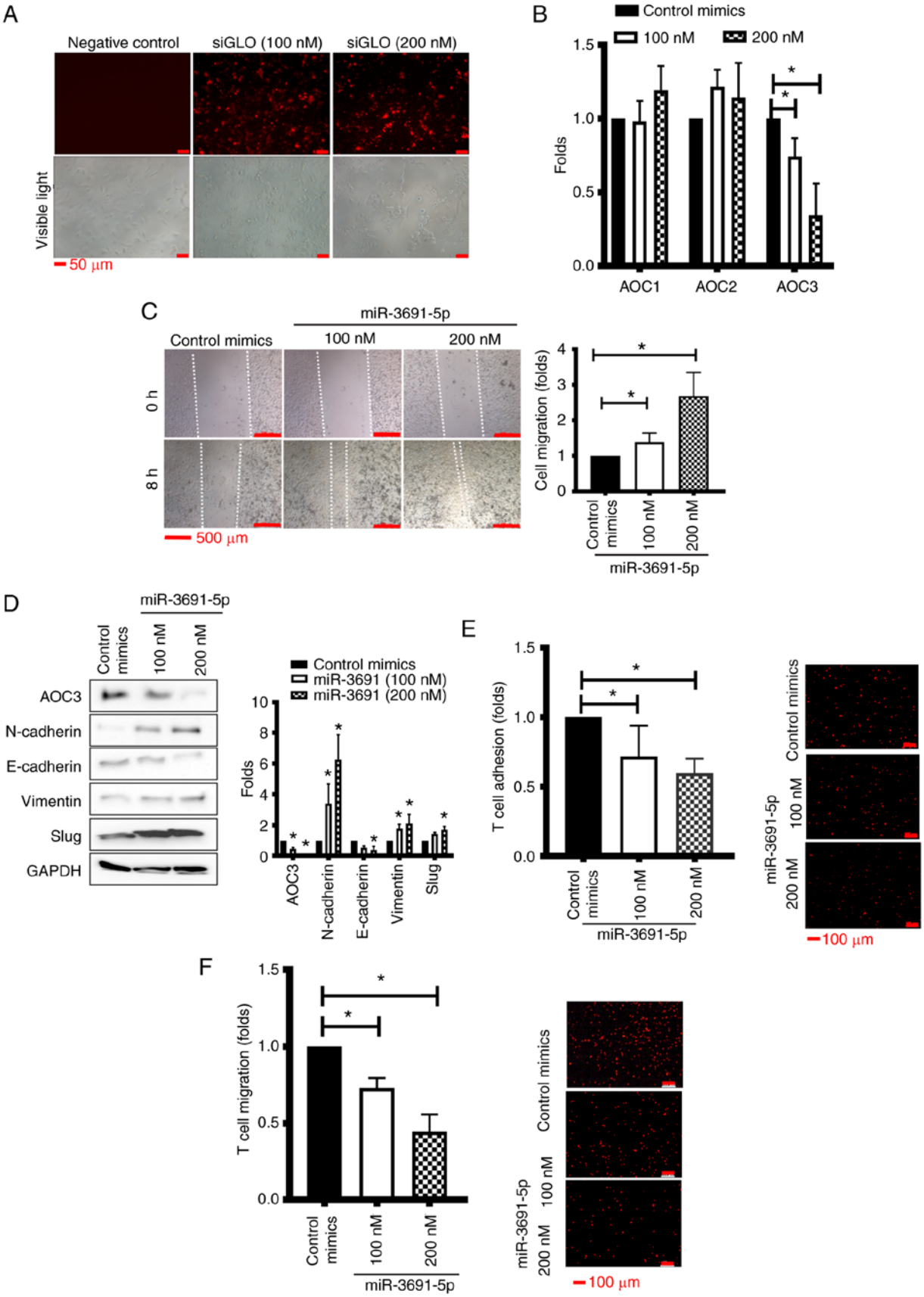

Figure 7. miR-3691 inhibits EMT through downregulation of *AOC3*. As predicted in Fig. 4E, miR-3691-5p was used to evaluate its effect on *AOC3*. (A) The transfection efficacy. (B) Low expression of *AOC3* but not *AOC1* nor *AOC2* after miR-3691-5p mimics transfection. (C) The miR-3691-5p-transfected CL1-5 cells were increased as indicated by wound-healing assay. (D) The EMT phenomenon shifted towards the mesenchymal characteristics as N-cadherin, vimentin and Slug were increased and epithelial characteristic indicated by E-cadherin was decreased after *AOC3* knockdown. (E) The *in vitro* cell adhesion of $CD4^+$ T cells on lung cancer cells was decreased after introduction of miR-3691-5p. (F) Moreover, the transendothelial migration assay revealed that less $CD4^+$ T cells were attracted to lung cancer cells compared with the control group. $^*P<0.05$. miR, microRNA; EMT, epithelial-mesenchymal transition; AOC, amine oxidase, copper containing 3.

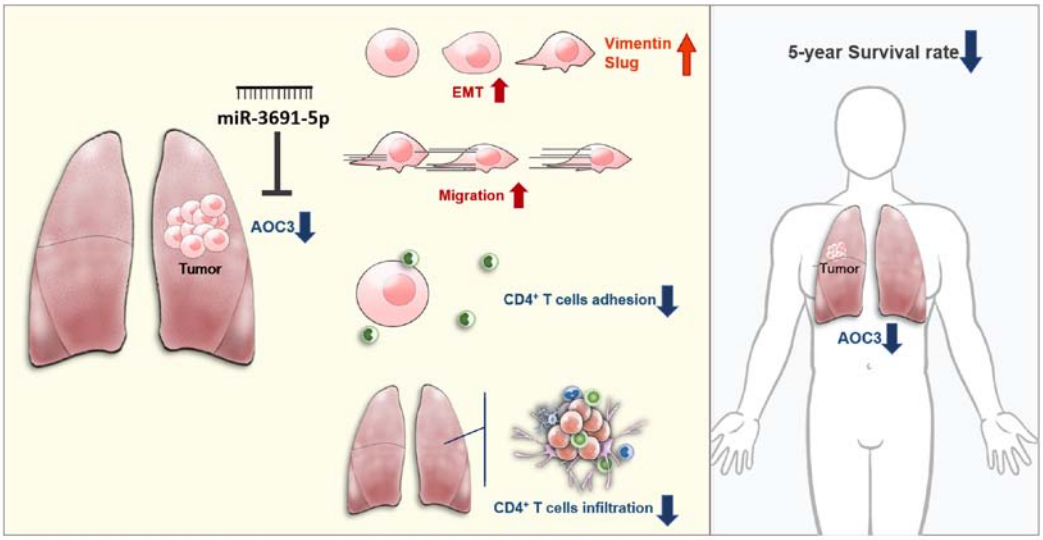

Figure 8. Proposed model of reduced AOC3 mediating lung cancer. The low expression of AOC3 mediated by miR-3691-5p in lung cancer conferred the potential of tumor cells to migrate and mesenchymal characteristics such as vimentin and Slug to increase. Moreover, low expression of AOC3 failed to recruit $CD4^+$ T cells to the tumor site *in vitro* and *in vivo*. These results may explain the reason why loss of AOC3 in tumor tissue leads to shorter 5-year survival time in lung cancer patients. AOC, amine oxidase, copper containing 3; miR, microRNA.

evaluate the miR-3691-5p-AOC3 axis in mediating the TIME in lung cancer, *in vitro* studies were performed. $CD4^+$ T-cell migration and adhesion to lung cancer cells were evaluated. As determined by a cell adhesion assay, $CD4^+$ T-cell attachment to lung cancer cells (CL1-5) was decreased after miR-3691-5p transfection in a dose-dependent manner (Fig. 7E). A transendothelial migration assay revealed that migration of $CD4^+$ T cells through endothelia was reduced in a dose-dependent manner with miR-3691-5p transfection (Fig. 7F). These results indicated that miR-3691-5p attenuated the recruitment of $CD4^+$ T cells. Collectively, it was indicated that miR-3691-5p regulated *AOC3* expression to perform its biological functions.

Discussion

The present study attempted to identify a novel factor affecting the different aspects of lung cancer pathogenesis. Through analysis of lung cancer patients via a high-throughput NGS tool, and the utilization of genomic data from different cohorts, the present study determined that AOC3 contributed to lung cancer pathogenesis. Different findings at both transcriptional and translational levels revealed that low levels of AOC3 were a critical factor contributing to cancer development. Low-level AOC3 facilitated mesenchymal transformation and decreased $CD4^+$ T-cell recruitment to lung cancer tumors. It was also revealed that AOC3 expression was under miR3691-5p epigenetic regulation. The strong negative association between AOC3 and the survival rate in patients indicated that it is a key factor involved in lung cancer, and that AOC3 could be a valuable target for drug development (Fig. 8). AOCs have different effects in different types of cancer (14,42-44,45,46). High levels of AOCs can act as oncogenes and confer worse clinical outcomes, such as AOC1 in gastric cancer (14) and AOC3 in human glioma (45). On the other hand, low levels of AOCs are associated with worse clinical outcomes, such as AOC3 in colorectal (42,47) and gastric cancer (46). Moreover, decreased AOC3 levels are correlated with lymph node and hepatic metastasis in colorectal cancer (47). The present study is the first one, to the best of our knowledge, which revealed that low-level AOC3 is the critical amine oxidase in lung cancer pathogenesis but not AOC1 or AOC2. Furthermore, miR-3691-5p regulation on AOC3 and its biological functions were defined. miR-3691-5p has been demonstrated to enhance migration and invasion in hepatocellular carcinoma (48). Low expression of AOC3 conferred poor clinical outcomes and lymph node metastasis, supporting the theory that AOC3 acts as a tumor suppressor in lung cancer. Biological function analyses revealed that AOC3 did not affect cell proliferation but that it did influence cell migration. The process of EMT is essential for the enhancement of cell migration (49). AOC3 knockdown enhanced mesenchymal characteristics as revealed by an increase in N-cadherin, vimentin and Slug and attenuated epithelial characteristics as revealed by a decrease in E-cadherin. Exogenous rhAOC3 reversed these mesenchymal patterns. This finding revealed that AOC3 is involved in the maintenance of epithelial characteristics to decrease the metastasis ability of lung cancer. For the first time, the present study has revealed the pathogenic roles of AOC3 in malignant cells and AOC3 *per se* providing a useful biomarker and prognostic factor in lung cancer patients for clinical diagnosis and treatment.

AOC3 contributes to both innate and acquired immunity (50). Endothelial AOC3 mediates the adhesion of tumor infiltration lymphocytes, lymphokine-activated killer cells and natural killer cells (51) in inflammatory tissue (52) and tumor tissue. An absence of AOC3 leads to a marked reduction in antigen-specific $CD4^+$ recruitment into the airway bronchial lymph nodes (50). In the present study, knockdown of AOC3 in lung cancer cells caused a reduction in $CD4^+$ T-cell extravasation through the endothelial layer and attachment to cancer cells. On the other hand, exogenous rhAOC3 increased transendothelial migration and enhanced $CD4^+$ T-cell attachment onto lung cancer cells. Furthermore, rmAOC3 facilitated $CD4^+$ T-cell recruitment to preexisting lung tumor in a mouse model. These results indicated that AOC3 could modulate the TIME in lung cancer cells, and it may be possible to potentiate

its effectiveness by immunotherapy. However, before reaching a definite conclusion, there are some limitations in the present study. Firstly, $CD4^+$ T cells were utilized as a recruiting immune cell to the lung. However, there are more immune cells such as dendritic cells and macrophages and consequently, further investigation may be necessary. Secondly, data from immunohistochemical staining for membrane-bound AOC3 in tumor tissues, which would limit the role of AOC3 in lung cancer, are lacking.

Collectively, the results of the present study confirmed the axis of miR-3691-5p-AOC3 as having a critical role in lung cancer via inhibiting EMT and migration and a determining factor for the recruitment of $CD4^+$ T cells to restore anticancer immunity in the TME. AOC3 expression in lung cancer specimens may provide valuable information for patient prognosis and could have valuable applications when determining a therapeutic strategy in immunotherapy/chemotherapy.

Acknowledgements

The authors would like to thank the CPTAC of UALCAN and the Human Protein Atlas who generated the data used in this publication. The authors would also like to thank the Center for Research Resources and Development in Kaohsiung Medical University for the assistance in Bioinformatics.

Funding

The present study was supported by the Ministry of Science and Technology (grant nos. 110-2314-B-037-124-MY3, 109-2314-B-037-091 and 108-2320-B-037-024-MY3), the Kaohsiung Medical University (grant no. KMU-DK108008), the Kaohsiung Medical University Hospital (grant nos. KMUH108-8R15, KMUH108-8R16 and MUH106-6T06) and the Kaohsiung Municipal Ta-Tung Hospital (grant nos. KMTTH-103-019 and KMTTH-105-051).

Availability of data and materials

The datasets generated and/or analyzed during the present study are not publicly available due to ongoing study in our laboratory but are available from the corresponding author on reasonable request.

Authors' contributions

CYC, YMT and YLH conceptualized the present study. SFJ, PHT and YCH provided the technical support, performed the experiments and acquired the data. CYC provided the software management and analyzed the data. YYC, JYH, WAC and IWC validated the results. KLW, YMT and YLH performed the formal analysis. YLH pursued the investigation and provided the resources. YMT, KLW and YLH performed data curation and interpreted the data. YMT and KLW wrote original draft. YYC and YLH wrote, reviewed and edited the final manuscript. IWC performed visualization of the imaging data. YLH supervised the study, was the project administrator and acquired the funding. YMT and YLH critically revised the manuscript for important intellectual content. All authors read and approved the final version of the manuscript.

Ethics approval and consent to participate

The protocol of the present study was approved (approval no. KMUH-IRB-20130054 and and KMUH-IRB-G(II)-20180021) by the Institutional Review Board of Kaohsiung Medical University Hospital (Kaohsiung, Taiwan) and written informed consents were acquired from all enrolled patients. All mice procedures were approved by the Institutional Animal Care and Use Committee at Kaohsiung Medical University (Kaohsiung, Taiwan).

Patient consent for publication

Not applicable.

Competing interests

The authors declare that they have no competing interests.

References

1. Ferlay J, Colombet M, Soerjomataram I, Mathers C, Parkin DM, Piñeros M, Znaor A and Bray F: Estimating the global cancer incidence and mortality in 2018: GLOBOCAN sources and methods. Int J Cancer 144: 1941-1953, 2019.
2. Siegel RL, Miller KD and Jemal A: Cancer statistics, 2019. CA Cancer J Clin 69: 7-34, 2019.
3. Arbour KC and Riely GJ: Systemic therapy for locally advanced and metastatic non-small cell lung cancer: A review. JAMA 322: 764-774, 2019.
4. Miller KD, Nogueira L, Mariotto AB, Rowland JH, Yabroff KR, Alfano CM, Jemal A, Kramer JL and Siegel RL: Cancer treatment and survivorship statistics, 2019. CA Cancer J Clin 69: 363-385, 2019.
5. National Lung Screening Trial Research Team: Lung Cancer Incidence and mortality with extended follow-up in the National lung screening trial. J Thorac Oncol 14: 1732-1742, 2019.
6. Elmore LW, Greer SF, Daniels EC, Saxe CC, Melner MH, Krawiec GM, Cance WG and Phelps WC: Blueprint for cancer research: Critical gaps and opportunities. CA Cancer J Clin 71: 107-139, 2021.
7. Binnewies M, Roberts EW, Kersten K, Chan V, Fearon DF, Merad M, Coussens LM, Gabrilovich DI, Ostrand-Rosenberg S, Hedrick CC, *et al*: Understanding the tumor immune microenvironment (TIME) for effective therapy. Nat Med 24: 541-550, 2018.
8. Duan Q, Zhang H, Zheng J and Zhang L: Turning cold into hot: Firing up the tumor microenvironment. Trends Cancer 6: 605-618, 2020.
9. Vakal S, Jalkanen S, Dahlstrom KM and Salminen TA: Human copper-containing amine oxidases in drug design and development. Molecules 25: 1293, 2020.
10. Mondovì B and Finazzi Agrò A: Structure and function of amine oxidase. Adv Exp Med Biol 148: 141-153, 1982.
11. Buffoni F and Ignesti G: The Copper-containing amine oxidases: Biochemical aspects and functional role. Mol Genet Metab 71: 559-564, 2000.
12. Boomsma F, Bhaggoe UM, van der Houwen AM and van den Meiracker AH: Plasma semicarbazide-sensitive amine oxidase in human (patho)physiology. Biochim Biophys Acta 1647: 48-54, 2003.
13. Salmi M and Jalkanen S: Vascular adhesion protein-1: A cell surface amine oxidase in translation. Antioxid Redox Signal 30: 314-332, 2019.
14. Xu F, Xu Y, Xiong JH, Zhang JH, Wu J, Luo J and Xiong JP: AOC1 Contributes to tumor progression by promoting the AKT and EMT pathways in gastric cancer. Cancer Manag Res 12: 1789-1798, 2020.
15. Lopes de Carvalho L, Bligt-Linden E, Ramaiah A, Johnson MS and Salminen TA: Evolution and functional classification of mammalian copper amine oxidases. Mol Phylogenet Evol 139: 106571, 2019.
16. Imamura Y, Kubota R, Wang Y, Asakawa S, Kudoh J, Mashima Y, Oguchi Y and Shimizu N: Human retina-specific amine oxidase (RAO): cDNA cloning, tissue expression, and chromosomal mapping. Genomics 40: 277-283, 1997.

17. Bonaiuto E, Lunelli M, Scarpa M, Vettor R, Milan G and Di Paolo ML: A structure-activity study to identify novel and efficient substrates of the human semicarbazide-sensitive amine oxidase/VAP-1 enzyme. Biochimie 92: 858-868, 2010.
18. Salmi M and Jalkanen S: A 90-kilodalton endothelial cell molecule mediating lymphocyte binding in humans. Science 257: 1407-1409, 1992.
19. Stankovic B, Bjørhovde HAK, Skarshaug R, Aamodt H, Frafjord A, Müller E, Hammarström C, Beraki K, Bækkevold ES, Woldbæk PR, *et al*: Immune cell composition in human non-small cell lung cancer. Front Immunol 9: 3101, 2019.
20. Oja AE, Piet B, van der Zwan D, Blaauwgeers H, Mensink M, de Kivit S, Borst J, Nolte MA, van Lier RAW, Stark R and Hombrink P: Functional heterogeneity of CD4$^+$ tumor-infiltrating lymphocytes with a resident memory phenotype in NSCLC. Front Immunol 9: 2654, 2018.
21. Rhodes DR, Yu J, Shanker K, Deshpande N, Varambally R, Ghosh D, Barrette T, Pandey A and Chinnaiyan AM: ONCOMINE: A cancer microarray database and integrated data-mining platform. Neoplasia 6: 1-6, 2004.
22. Chandrashekar DS, Bashel B, Balasubramanya SAH, Creighton CJ, Ponce-Rodriguez I, Chakravarthi BVSK and Varambally S: UALCAN: A portal for facilitating tumor subgroup gene expression and survival analyses. Neoplasia 19: 649-658, 2017.
23. Su LJ, Chang CW, Wu YC, Chen KC, Lin CJ, Liang SC, Lin CH, Whang-Peng J, Hsu SL, Chen CH and Huang CY: Selection of DDX5 as a novel internal control for Q-RT-PCR from microarray data using a block bootstrap re-sampling scheme. BMC Genomics 8: 140, 2007.
24. Okayama H, Kohno T, Ishii Y, Shimada Y, Shiraishi K, Iwakawa R, Furuta K, Tsuta K, Shibata T, Yamamoto S, *et al*: Identification of genes upregulated in ALK-positive and EGFR/KRAS/ALK-negative lung adenocarcinomas. Cancer Res 72: 100-111, 2012.
25. Landi MT, Dracheva T, Rotunno M, Figueroa JD, Liu H, Dasgupta A, Mann FE, Fukuoka J, Hames M, Bergen AW, *et al*: Gene expression signature of cigarette smoking and its role in lung adenocarcinoma development and survival. PLoS One 3: e1651, 2008.
26. Beer DG, Kardia SL, Huang CC, Giordano TJ, Levin AM, Misek DE, Lin L, Chen G, Gharib TG, Thomas DG, *et al*: Gene-expression profiles predict survival of patients with lung adenocarcinoma. Nat Med 8: 816-824, 2002.
27. Stearman RS, Dwyer-Nield L, Zerbe L, Blaine SA, Chan Z, Bunn PA Jr, Johnson GL, Hirsch FR, Merrick DT, Franklin WA, *et al*: Analysis of orthologous gene expression between human pulmonary adenocarcinoma and a carcinogen-induced murine model. Am J Pathol 167: 1763-1775, 2005.
28. Selamat SA, Chung BS, Girard L, Zhang W, Zhang Y, Campan M, Siegmund KD, Koss MN, Hagen JA, Lam WL, *et al*: Genome-scale analysis of DNA methylation in lung adenocarcinoma and integration with mRNA expression. Genome Res 22: 1197-1211, 2012.
29. Garber ME, Troyanskaya OG, Schluens K, Petersen S, Thaesler Z, Pacyna-Gengelbach M, van de Rijn M, Rosen GD, Perou CM, Whyte RI, *et al*: Diversity of gene expression in adenocarcinoma of the lung. Proc Natl Acad Sci USA 98: 13784-13789, 2001.
30. Hou J, Aerts J, den Hamer B, van Ijcken W, den Bakker M, Riegman P, van der Leest C, van der Spek P, Foekens JA, Hoogsteden HC, *et al*: Gene expression-based classification of non-small cell lung carcinomas and survival prediction. PLoS One 5: e10312, 2010.
31. Wachi S, Yoneda K and Wu R: Interactome-transcriptome analysis reveals the high centrality of genes differentially expressed in lung cancer tissues. Bioinformatics 21: 4205-4208, 2005.
32. Bhattacharjee A, Richards WG, Staunton J, Li C, Monti S, Vasa P, Ladd C, Beheshti J, Bueno R, Gillette M, *et al*: Classification of human lung carcinomas by mRNA expression profiling reveals distinct adenocarcinoma subclasses. Proc Natl Acad Sci USA 98: 13790-13795, 2001.
33. Uhlen M, Zhang C, Lee S, Sjöstedt E, Fagerberg L, Bidkhori G, Benfeitas R, Arif M, Liu Z, Edfors F, *et al*: A pathology atlas of the human cancer transcriptome. Science 357: eaan2507, 2017.
34. Gyorffy B, Surowiak P, Budczies J and Lanczky A: Online survival analysis software to assess the prognostic value of biomarkers using transcriptomic data in non-small-cell lung cancer. PLoS One 8: e82241, 2013.
35. Mende DR, Letunic I, Maistrenko OM, Schmidt TS, Milanese A, Paoli L, Hernández-Plaza A, Orakov AN, Forslund SK, Sunagawa S, *et al*: proGenomes2: An improved database for accurate and consistent habitat, taxonomic and functional annotations of prokaryotic genomes. Nucleic Acids Res 48: D621-D625, 2020.
36. Sticht C, De La Torre C, Parveen A and Gretz N: miRWalk: An online resource for prediction of microRNA binding sites. PLoS One 13: e0206239, 2018.
37. Enright AJ, John B, Gaul U, Tuschl T, Sander C and Marks DS: MicroRNA targets in Drosophila. Genome Biol 5: R1, 2003.
38. Chen Y and Wang X: miRDB: An online database for prediction of functional microRNA targets. Nucleic Acids Res 48: D127-D131, 2020.
39. Ke HL, Li WM, Lin HH, Hsu WC, Hsu YL, Chang LL, Huang CN, Li CC, Chang HP, Yeh HC, *et al*: Hypoxia-regulated MicroRNA-210 overexpression is associated with tumor development and progression in upper tract urothelial carcinoma. Int J Med Sci 14: 578-584, 2017.
40. Livak KJ and Schmittgen TD. Analysis of relative gene expression data using real-time quantitative PCR and the 2(-Delta Delta C(T)) method. Methods 25: 402-408, 2001.
41. Shao L, Li H, Chen J, Song H, Zhang Y, Wu F, Wang W, Zhang W, Wang F, Li H and Tang D: Irisin suppresses the migration, proliferation, and invasion of lung cancer cells via inhibition of epithelial-to-mesenchymal transition. Biochem Biophys Res Commun 485: 598-605, 2017.
42. Ward ST, Weston CJ, Shepherd EL, Hejmadi R, Ismail T and Adams DH: Evaluation of serum and tissue levels of VAP-1 in colorectal cancer. BMC Cancer 16: 154, 2016.
43. Sun WY, Choi J, Cha YJ and Koo JS: Evaluation of the expression of amine oxidase proteins in breast cancer. Int J Mol Sci 18: 2775, 2017.
44. Kostoro J, Chang SJ, Clark Lai YC, Wu CC, Chai CY and Kwan AL: Overexpression of vascular adhesion protein-1 is associated with poor prognosis of astrocytomas. APMIS 124: 462-468, 2016.
45. Chang SJ, Tu HP, Lai YCC, Luo CW, Nejo T, Tanaka S, Chai CY and Kwan AL: Increased vascular adhesion protein 1 (VAP-1) levels are associated with alternative M2 macrophage activation and poor prognosis for human gliomas. Diagnostics (Basel) 10: 256, 2020.
46. Yasuda H, Toiyama Y, Ohi M, Mohri Y, Miki C and Kusunoki M: Serum soluble vascular adhesion protein-1 is a valuable prognostic marker in gastric cancer. J Surg Oncol 103: 695-699, 2011.
47. Toiyama Y, Miki C, Inoue Y, Kawamoto A and Kusunoki M: Circulating form of human vascular adhesion protein-1 (VAP-1): Decreased serum levels in progression of colorectal cancer and predictive marker of lymphatic and hepatic metastasis. J Surg Oncol 99: 368-372, 2009.
48. Du W, Zhang X and Wan Z: miR-3691-5p promotes hepatocellular carcinoma cell migration and invasion through activating PI3K/Akt signaling by targeting PTEN. Onco Targets Ther 12: 4897-4906, 2019.
49. Leggett SE, Hruska AM, Guo M and Wong IY: The epithelial-mesenchymal transition and the cytoskeleton in bioengineered systems. Cell Commun Signal 19: 32, 2021.
50. Dunkel J, Aguilar-Pimentel JA, Ollert M, Fuchs H, Gailus-Durner V, de Angelis MH, Jalkanen S, Salmi M and Veres TZ: Endothelial amine oxidase AOC3 transiently contributes to adaptive immune responses in the airways. Eur J Immunol 44: 3232-3239, 2014.
51. Irjala H, Salmi M, Alanen K, Grénman R and Jalkanen S: Vascular adhesion protein 1 mediates binding of immunotherapeutic effector cells to tumor endothelium. J Immunol 166: 6937-6943, 2001.
52. Stolen CM, Marttila-Ichihara F, Koskinen K, Yegutkin GG, Turja R, Bono P, Skurnik M, Hänninen A, Jalkanen S and Salmi M: Absence of the endothelial oxidase AOC3 leads to abnormal leukocyte traffic in vivo. Immunity 22: 105-115, 2005.